

Rotordynamic prediction of mode order transition when rotor has an overhang

Konstantin Shaposhnikov, HONG Jie, ZHANG Da-yi, MA Yan-hong
(School of Energy and Power Engineering,
Beijing University of Aeronautics and Astronautics, Beijing 100191, China)

Abstract: Nowadays rotating machinery grows and develops extremely fast due to its multi-branch application. Although the fields of rotordynamics and rotor balancing had a strong background based on previous experience in order to perform efficient and safe operation for the rotating machines, still there are problems which are hard to be dealt with in some special cases. One of them is balancing of the rotor with huge overhang. Rotor with overhang is inherent to have console modes, which previously often were observed separately from the other modes in rotordynamic literature. In such a way console modes, their behavior, order of appearance and interaction with other modes were described in current paper in more details. Obtained results confirmed that console modes obey the principle of orthogonality in the same way as all other modes and hence could be efficiently balanced using modal balancing method. Simulation results revealed likelihood of such phenomena as modes order transition, when the rotor has an overhang. As a consequence perfectly balanced console rotor could not be so due to modes order transition effect when the bearing stiffness in situ differs from bearing stiffness of balancing equipment. Described results will be useful for engineers who are involved in area of rotating machinery vibration tuning for the rotor with huge overhang and benefit them to recognize these modes efficiently and to perform balancing successfully.

Key words: rotordynamics; turbomachinery; rotor with overhang; console modes; balancing

CLC number: V231

Document code: A

Nowadays rotordynamic field has a strong background and scientific support based on computer predictions, modeling and simulation, but still there are problems that are hard to be dealt with in some special case. One of them is balancing of the rotors with huge overhangs. Even though the rotor balancing facilities were highly improved and upgraded since the 1970s when they first appeared but still they are only a tool in hands of modern engineers and more important usually is their qualification and experience.

Rotors with huge overhangs today are widespread not only among gas turbines, where they probably first appeared, but also in power machinery for the rotors of generators. And as a consequence, they are usual “guests” at the high speed balancing facilities, where the engineers with “sweat and blood” developed methods for

their efficient and effective balancing^[1].

Main principles of balancing and balancing of the rotors with huge overhangs for different types of power rotors are widely described in Ref. [2-8]. Specific case for the gas turbine rotor was described in Ref. [9], where engineers while performing balancing, faced the problem of amplitude hysteresis. The main reason was an increase of kinetic energy for the rotor working near the console resonant mode, where increase was forced not only by rotational component but also by means of console precession motion.

As it was pointed out in Ref. [10], still problems could be faced, when there is no clear understanding how to deal with the rotor whose main feature is a huge overhang, and hence most contemporary and effective modern technique to deal with the overhang rotor were described in

details on the example of the problem rotor. At the same time this paper mentioned likelihood of such phenomena as the order change for the console mode shapes compare with the other modes. The midspan rotor mode shapes are clearly described and many time observed in rotordynamic literatures^[11-14], while console modes are usually ignored.

Since the limited number of papers about console modes behavior and their importance for efficient balancing of the rotors, the purpose of the current paper is to give further explanation about them, their behavior and order appearance, while at the same time outline possible mistakes in their identification, in order not to confuse with the other modes.

1 Mode shapes description

In rotordynamic literature console modes are often called “L-modes”^[1,3] mainly because of their similarity with the abovementioned shape of the letter. General view of a typical console mode shape is shown in Fig. 1. When the rotor is inherent to have such feature as an overhang mainly because of construction elements such as couplings as it is usual for power rotors or disk with blades or fan as for turbofan aircraft engine low-pressure rotor, then the console modes will definitely appear and give its influence on rotor-dynamic behavior of the full rotor. Console modes are usually called those modes when vibration

amplitude and deflection of the overhang end of the rotor are significantly higher than that of the other parts. In contrast, the modes when the significant deflection and vibration are inherent to the parts of the rotor between bearings are called midspan modes.

But as a result console modes are usually observed separately from the other modes or midspan modes. In accordance with principle of the orthogonality, it is assumed that the work of inertial forces when vibrating on one mode shape on displacement to the other mode is always equal to zero. That denotes the energy independence of the mode shapes, meaning that the transfer of the vibration motion energy from one mode to the other is impossible.

To demonstrate the behavior of the midspan mode shapes a critical speed map was build for the simple shaft with two bearings, designed in the rotordynamic software DyRoBeS (Fig. 2).

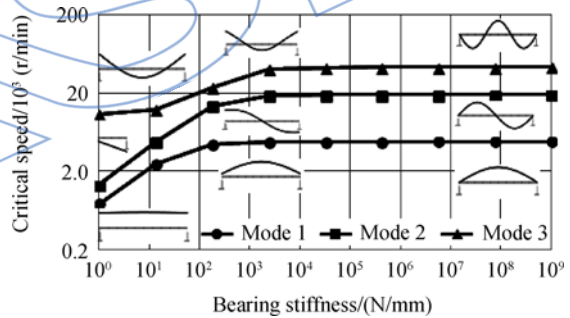


Fig. 2 Critical speed map for simple shaft with two bearings

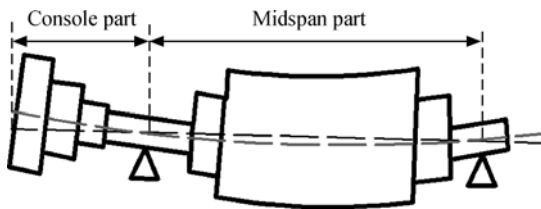


Fig. 1 Console mode shape

The shaft was modeled using beam elements, where the degree of freedom (DOF) are defined by $\mathbf{q} = [u_x, u_y, \theta_x, \theta_y]^T$, hence each element was modeled by 8 DOFs with two lateral translations (u_x, u_y) and two bending rotations (θ_x, θ_y). The stiffness matrix for each element is

$$\mathbf{K} = \frac{EI}{L^3} \begin{bmatrix} 12 & 0 & 0 & 6L & -12 & 0 & 0 & 6L \\ 0 & 12 & -6L & 0 & 0 & -12 & -6L & 0 \\ 0 & -6L & 4L^2 & 0 & 0 & 6L & 2L^2 & 0 \\ 6L & 0 & 0 & 4L^2 & -6L & 0 & 0 & 2L^2 \\ -12 & 0 & 0 & -6L & 12 & 0 & 0 & -6L \\ 0 & -12 & 6L & 0 & 0 & 12 & 6L & 0 \\ 0 & -6L & 2L^2 & 0 & 0 & 6L & 4L^2 & 0 \\ 6L & 0 & 0 & 2L^2 & -6L & 0 & 0 & 4L^2 \end{bmatrix} \quad (1)$$

where E is the elasticity modulus; $I = \pi r^4/4$ is area moment of inertia for the shaft segment; r is radius and L is length of the element section.

Mass matrix for each element is

$$\mathbf{M} = \frac{m}{420} \begin{bmatrix} 156 & 0 & 0 & 22L & 54 & 0 & 0 & -13L \\ 0 & 156 & -22L & 0 & 0 & 54 & 13L & 0 \\ 0 & -22L & 4L^2 & 0 & 0 & -13L & -3L^2 & 0 \\ 22L & 0 & 0 & 4L^2 & 13L & 0 & 0 & -3L^2 \\ 54 & 0 & 0 & 13L & 156 & 0 & 0 & -22L \\ 0 & 54 & -13L & 0 & 0 & 156 & 22L & 0 \\ 0 & 13L & -3L^2 & 0 & 0 & 22L & 4L^2 & 0 \\ -13L & 0 & 0 & -3L^2 & -22L & 0 & 0 & 4L^2 \end{bmatrix} \quad (2)$$

where m is the mass of one element. The bearing stiffness and damping matrices are

$$\mathbf{K}_b = \begin{bmatrix} K_{xx} & K_{xy} & 0 & 0 \\ K_{yx} & K_{yy} & 0 & 0 \\ 0 & 0 & 0 & 0 \\ 0 & 0 & 0 & 0 \end{bmatrix} \quad (3)$$

$$\mathbf{C}_b = \begin{bmatrix} C_{xx} & C_{xy} & 0 & 0 \\ C_{yx} & C_{yy} & 0 & 0 \\ 0 & 0 & 0 & 0 \\ 0 & 0 & 0 & 0 \end{bmatrix} \quad (4)$$

At the same time to simplify the calculations cross-coupled component in abovementioned formulas (3)–(4) were neglected.

It could be seen from the obtained results that in area of the soft bearings the shaft behaves like a rigid body, while with increase of the bearing stiffness the critical speeds of the modes also increase. However in area of rigid bearings the shaft behaves like a flexible body and further increase of bearing stiffness do not influence so much on increase of the critical speeds. Obtained results correspond to classical definition for the lateral mode shapes where the order of the mode shapes corresponds to the rule: first goes first classical midspan mode shape, then follows second midspan mode shape, after-third mode shape and etc. In other words, the order of the mode shapes appearance is constant and never changes.

2 Verification of orthogonality principle for console modes

Back to principle of orthogonality between

the mode shapes, it could be assumed that the inertial forces are proportional to product of oscillating masses and shaft deflections, while the deflections at the moment of maximum deviation are equal to amplitudes. Hence the orthogonal condition for the n -th and m -th main modes could be written as^[15]

$$\sum_{i=1}^k m_i A_i^n A_i^m = 0 \quad (5)$$

where m_i is the mass of the shaft's i -th element; A_i^n is deflection for the shaft's element corresponding to the n -th mode; A_i^m is deflection for the shaft's element corresponding to the m -th mode.

To demonstrate the effect of orthogonal condition several models of simple shafts were created (Table 1), and then numerically calculated using abovementioned formula when distributed unbalances all along the shaft body for the first five ordinal modes were given in the rotordynamic software. Simple models were specifically chosen in order to clearly describe abovementioned effect. One shaft was able to have only midspan modes while the others were inherent to have both midspan and console modes. During the calculations unbalances were given for the specific modes and then its influence on the other modes was evaluated and compared. For that purpose shaft deflections for the specific modes were examined. All shafts were modeled to be made of steel and consisted from equal segments with $D=0.01$ m and $L=0.05$ m. Bearings for all models were considered as rigid.

Results of numerical simulations were summarized in form of Table 2—Table 5. Number in each cell of each table represents the ratio where in numerator are shaft displacements which correspond to ordinal modes and in denominator are shaft displacements for mode by which unbalance was distributed along the body of the shaft.

Obtained results for the two bearing shaft (Table 2) showed a good agreement with theoretical background; given distributed unbalance influenced only corresponding mode, without

any influence on the other modes, and hence in every case only specific mode was excited. For the model with overhang (Table 3) distributed unbalance by specific mode influenced on this mode mainly and at the same time small disturbance influence on other modes was fixed. The reason of this influence on the other modes was due to errors in unbalance distribution assumption because of the FEM software limitations, model discrete and round off errors. Nevertheless unbalance, which is given for the specific mode, influenced generally only on this certain mode.

Table 1 Simple shaft models overview





No.	Model view	Description	Modes excited
1		Two bearing shaft, 10 segments	Only midspan modes
2		Two bearing shaft with one overhang, 13 segments	Have midspan+ console modes
3		Two bearing shaft with two equal overhangs, 16 segments	
4		Two bearing shaft with two not equal overhangs, 15 segments	

Table 2 Model 1 (two bearing shaft)

Unbalance distribution	Mode number				
	1	2	3	4	5
Mode 1	1	0	0	0	0
Mode 2	0	1	0	0	0
Mode 3	0	0	1	0	0
Mode 4	0	0	0	1	0
Mode 5	0	0	0	0	1

Table 3 Model 2 (two bearing shaft with one overhang)

Unbalance distribution	Mode number				
	1	2	3	4	5
Mode 1	1.000	0.012	0.014	0.012	0.026
Mode 2	0.043	1.000	0.052	0.045	0.097
Mode 3	0.013	0.014	1.000	0.013	0.028
Mode 4	0.013	0.013	0.014	1.000	0.022
Mode 5	0.028	0.029	0.030	0.023	1.000

Table 4 Model 3 (two bearing shaft with two equal overhangs)

Unbalance distribution	Mode number				
	1	2	3	4	5
Mode 1	1.000	0	0.019	0	0.020
Mode 2	0	1.000	0	0.057	0
Mode 3	0.048	0	1.000	0	0.052
Mode 4	0	0.023	0	1.000	0
Mode 5	0.024	0	0.026	0	1.000

Table 5 Model 4 (two bearing shaft with two not equal overhangs)

Unbalance distribution	Mode number				
	1	2	3	4	5
Mode 1	1.000	0.007	0.016	0.005	0.023
Mode 2	0.026	1.000	0.002	0.044	0.016
Mode 3	0.050	0.001	1.000	0.045	0.083
Mode 4	0.018	0.043	0.052	1.000	0.056
Mode 5	0.024	0.004	0.028	0.016	1.000

When the abovementioned model was transformed to a rotor with two equal overhangs (Table 4), and hence became symmetric, the effect was more evident. Given distributed unbalance influenced on the corresponding modes and at the same time some small influence on other modes was also received. But it should be pointed out that unbalances distributed by “odd” modes had influence only on other “odd” modes, but not on the “even” modes. And vice versa unbalances distributed by “even” modes affected on other “even” modes. When the model again became asymmetric like in case with model, that has two but not equal overhangs (Table 5), the influence of distributed unbalance excited corresponding modes, but there was also some small disturbance on the other modes.

Hence it could be seen that several modes of the rotor were considered including console modes and all of them obey the principle of orthogonality. So it could be concluded that according to classical definition the balancing of the flexible rotor could be performed considering its bending mode shapes, caused by inertial forces that change with the speed increase. Then based on that principle, balancing of the flexible rotor could be implemented separately for each of the mode, step by step eliminating every mode shape at the corresponding critical speed or near it. Since console modes obey the principle of orthogonal, what was proven by calculation, they should not be considered separately from the other modes.

3 Phenomenon of console mode transition

Another interesting phenomenon that should be examined in more details, related to the console modes and which could happen when the rotor has an overhang. The physical definition of it is the change of the console mode shapes order or modes transition when they can wedge between the other modes.

3.1 Critical speeds and mode shapes

For the demonstration purpose in this case more complex model of the rotor on two bear-

ings with the disk on console was considered. The shaft diameter was 20 mm, length of console 65 mm and the ratio of the full rotor length to console length was equal to $L/L_{\text{cons}} \approx 8$. The disk mass was almost 2 kg with outer diameter of 150 mm and length of 15 mm. The rotor was also modeled using beam elements in rotordynamic software. In Fig. 3(a) the critical speed map for abovementioned model rotor on two bearings with overhang disk is shown, obtained in rotordynamic software. Table 6 sum up the results of calculation for the rotor critical speeds and its mode shapes on the soft and rigid bearings. It is known that increase of bearing stiffness usually brings to increase of the critical speeds for the modes, but it is interesting to point out that mode 2 has a small hump directed to mode 1 in the zone $10^3 - 10^4$ N/mm of bearing stiffness (emphasized by the black oval). Mode shape analysis of the critical speeds for the same rotor for different bearing stiffness (Table 6) showed that mode 1 which was initially a console mode on the soft bearings with increase of bearing stiffness transformed to the rotor first midspan mode on the rigid bearings, while at the same time the first midspan mode which was initially a second ordinal mode on the soft bearings, became a console mode with a midspan bending by the mode 1.

Hence it could be concluded from the Fig. 3 (a) that the modes with different mode shapes were combined in one line, probably because the software could not recognize the mode shapes and while building critical speed map only connects the points with the same serial numbers. That brings to decision that this map could have some inaccuracy and hence should be clarified taking into account mode shape analysis.

As a result the current critical speed map was rebuilt considering the mode shapes for each mode, and critical speeds with similar mode shapes were combined and tagged with the same markers in Fig. 3(b). Mode shapes for the region of bearing stiffness $10^3 - 10^4$ N/mm are shown in Table 7. From engineering point of view rebuilt

Table 6 Undamped critical speeds and mode shapes for overhang rotor

No.	Bearing stiffness/(N/mm)				
	10^3	10^4	10^5	10^7	10^9
Mode 1	5066 r/min (84.43 Hz)	9311 r/min (155.19 Hz)	9834 r/min (163.9 Hz)	9884 r/min (164.74 Hz)	9884 r/min (164.74 Hz)
Mode 2	9597 r/min (159.96 Hz)	15289 r/min (254.82 Hz)	22727 r/min (378.78 Hz)	24685 r/min (411.42 Hz)	24707 r/min (411.79 Hz)
Mode 3	26625 r/min (443.75 Hz)	43995 r/min (733.25 Hz)	53817 r/min (896.96 Hz)	58313 r/min (971.88 Hz)	58374 r/min (972.92 Hz)

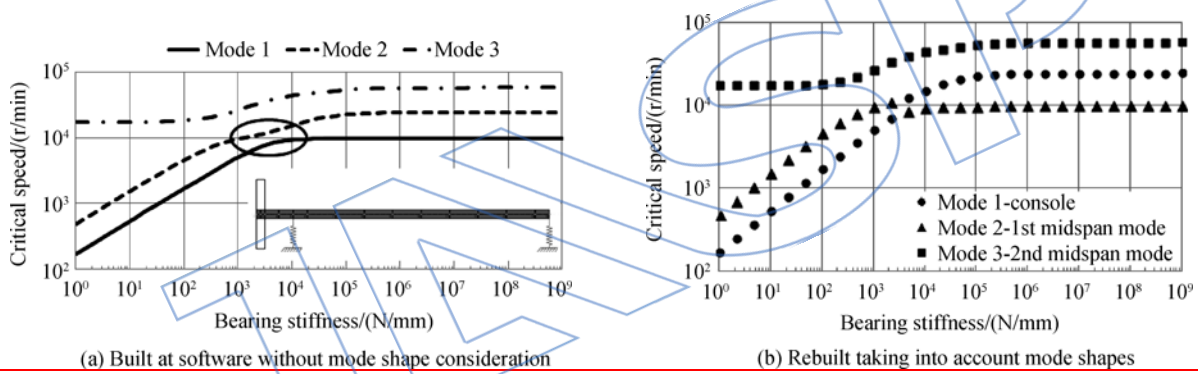


Fig. 3 Critical speed map

Table 7 Detailed observation of undamped critical speeds and mode shapes for overhang rotor in range of bearing stiffness $10^3 - 10^4$ N/mm

No.	Bearing stiffness/(N/mm)				
	10^3	2×10^3	5×10^3	8×10^3	10^4
Mode 1	5066 r/min (84.43 Hz)	6075 r/min (111.74 Hz)	8604 r/min (143.40 Hz)	9144 r/min (150.40 Hz)	9311 r/min (155.19 Hz)
Mode 2	9597 r/min (159.96 Hz)	10278 r/min (178.79 Hz)	12789 r/min (213.14 Hz)	14418 r/min (240.30 Hz)	15289 r/min (254.82 Hz)
Mode 3	26625 r/min (443.75 Hz)	32368 r/min (539.46 Hz)	39885 r/min (664.74 Hz)	42811 r/min (713.52 Hz)	43995 r/min (733.25 Hz)

critical speed map is more informative since it gives the possibility to understand mode shapes behavior with the changes of bearing stiffness and associates the mode shapes with critical speeds. Observed interspace of bearing stiffness ($10^3 - 10^4$ N/mm) could be called mode shapes transition region. It should be pointed out that there is no crossing point between the modes, since two modes cannot realize for the same bearing stiffness, but mode shapes transition could happen. At the same time one cannot simply define the exact bearing stiffness when the transition happens due to the difficulties in mode shapes recognition and time-consuming calculations. Nevertheless rebuilt map can help to identify the region where transition can occur and hence help to choose necessary bearing stiffness in order not to have two modes close to each other, when one of them is console mode.

Figure 4 shows the potential energy distribution for the first two modes that were mentioned in Fig. 3(b). It could be seen that for the first ordinal mode (Fig. 4(a)) for the bearing stiffness 10^3 N/mm most of the energy is concentrated on the front bearing, due to high motion of the console end. At the same time for the bearing stiffness 10^4 N/mm most of the strain energy will be concentrated on the shaft, confirming that it is a bending mode, because due to the mode shapes transition it is already a first midspan mode. Results for the second ordinal mode (Fig. 4 (b)) could be observed in the same way: for the bearing stiffness 10^3 N/mm most of the energy is on the shaft, affirming that it is a bending mode, but increase of bearing stiffness brings to increase of the strain energy on the front bearing, now confirming that console mode became second ordinal mode.

This situation with the mode transition could be explained in this way: the natural frequencies of the midspan modes depend upon the bearing stiffness but the order of their appearance always remains constant, what was proven by simulation results (Fig. 2). Console modes are more unique: their natural frequencies have a

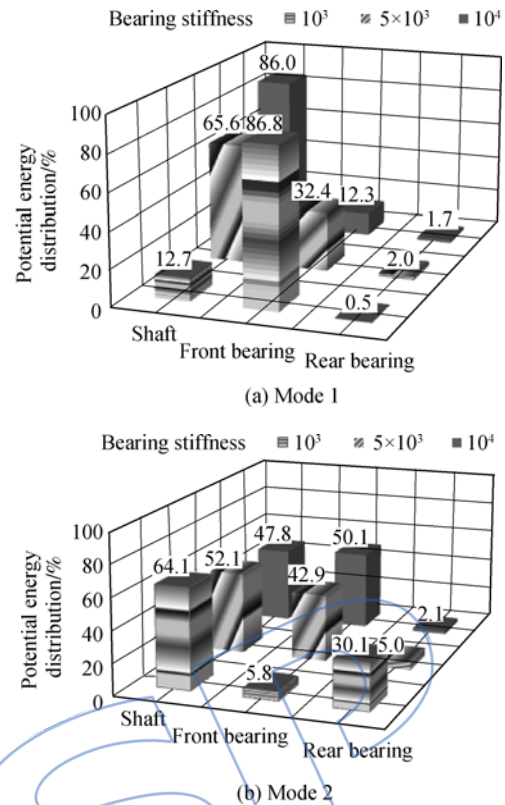


Fig. 4 Potential energy distribution

more complicated dependence upon the parameters of the rotor-bearing system.

3.2 Principles of modeling

It should be noted that console modes natural frequency depends more on the rotor body stiffness and specifically regulated by the stiffness of the clamped end, i. e. by the shaft stiffness at the bearing location. Figure 5 shows a principle of modeling for the typical rotor-bearing structure in rotordynamic software emphasizing connection of the console part with midspan

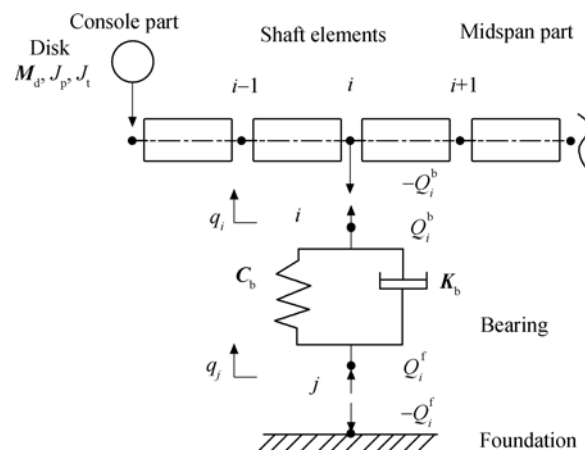


Fig. 5 Rotor-bearing connection schematic model

part in the region of bearing.

In stationary frame of references the equation of motion for the disk could be written as

$$\mathbf{M}_d \ddot{\mathbf{q}}_d + \Omega \mathbf{G}_d \dot{\mathbf{q}}_d = \Omega^2 \mathbf{F}_u + \mathbf{F}_s - \mathbf{Q}_s^d + \mathbf{Q}_g^I \quad (6)$$

where \mathbf{M}_d , \mathbf{G}_d are the mass and gyroscopic matrix for the disk, Ω is the rotating speed; \mathbf{F}_u is vector of unbalance force, \mathbf{F}_s is the vector of uni-directional load from the shaft, \mathbf{Q}_s^d is the vector of interactive forces and moments at common nodes of disk and shaft, \mathbf{Q}_g^I is the vector of inertia forces and moments for the disk relative to foundation.

The equation of motion for the bearing could be written as

$$\mathbf{C}_b \dot{\mathbf{q}}_b + \mathbf{K}_b \mathbf{q}_b = -\mathbf{Q}_b + \mathbf{Q}_f \quad (7)$$

where \mathbf{C}_b , \mathbf{K}_b are the bearing damping and stiffness matrix; \mathbf{Q}_b is the vector of interactive forces acting at the common nodes of rotor and bearing elements; \mathbf{Q}_f is the vector of interactive forces acting at the common nodes of bearing and foundation elements.

Then the equation of motion for the full rotor system will be

$$\mathbf{M}_\Sigma \ddot{\mathbf{q}} + (\mathbf{C}_\Sigma + \omega \mathbf{G}) \dot{\mathbf{q}} + \mathbf{K}_\Sigma \mathbf{q} = \Omega^2 \mathbf{F}_u + \mathbf{F}_f + \mathbf{Q}_d + \mathbf{Q}_b \quad (8)$$

where \mathbf{M}_Σ , \mathbf{C}_Σ are the total mass and damping matrixes; \mathbf{G} is the gyroscopic matrix; \mathbf{K}_Σ is the total stiffness matrix for the system; \mathbf{F}_u is vector of unbalance forces; \mathbf{F}_f is vector of transmitted forces into the bearing; \mathbf{Q}_d is vector of interactive forces at the node of the disk; \mathbf{Q}_b is vector of interactive forces at the nodes of bearings.

3.3 Separate calculation of substructures for complete rotor

At the same time the rotor with overhang structure can be considered as a rotor train structure which consists of midspan part (rotor on two bearings) and console part (include overhang with one free end and one end on the bearing)(Fig. 6). Hence the mode shapes and natural frequencies of the full structure would be influenced by the manner and the mode shapes of its main parts.

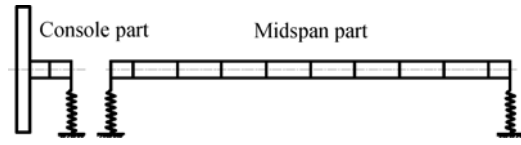


Fig. 6 Model separate calculation

Equation of motion for the midspan part could be built easily combining formulas (1) – (4). For the console part since it consists from the shaft elements and disk which is modeled as a lumped mass, the disk mass matrix should be added to the shaft matrix

$$\mathbf{M}_d = \begin{bmatrix} m_d & 0 & 0 & 0 \\ 0 & m_d & 0 & 0 \\ 0 & 0 & J_d & 0 \\ 0 & 0 & 0 & J_d \end{bmatrix} \quad (9)$$

where m_d is the mass of the disk and $J_d = \frac{m}{12} \cdot (3R_d^2 + h^2)$ is the mass moment of inertia; h is the width and R_d is the radius of the disc.

Besides gyroscopic effect should be taken into account, thus the damping matrix for the disk will be

$$\mathbf{C}_d = \begin{bmatrix} 0 & 0 & 0 & 0 \\ 0 & 0 & 0 & 0 \\ 0 & 0 & 0 & J_p \omega \\ 0 & 0 & J_p \omega & 0 \end{bmatrix} \quad (10)$$




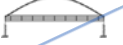






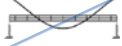
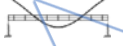
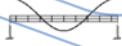
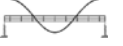
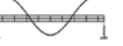
where $\omega = 2\pi n/60$ is the driving frequency with n rotation speed in r/min; $J_p = \frac{1}{2} m_d R_d^2$ is the polar mass moment of inertia.

In such a way critical speeds for console part (Table 8) and midspan part (Table 9) were calculated separately in order to estimate its influence and compare with results for the full rotor. While calculation of the console part, only one bearing was added at the console end, besides rotational displacements in vertical and horizontal direction were constrained in the bearing node location. Console part of the rotor when considered separately will also have numerous mode shapes, natural frequencies and associated with them critical speeds but the main interest in our case was only to the first ordinal mode.

Table 8 Undamped critical speeds for console part of mode 1

Case	Bearing stiffness/(N/mm)				
	10^3	2×10^3	5×10^3	8×10^3	10^4
Non-rotating	6 307 r/min	8 742 r/min	12 985 r/min	15 482 r/min	16 525 r/min
	105. 12 Hz	145. 70 Hz	216. 42 Hz	256. 86 Hz	275. 41 Hz
With rotation	6 315 r/min	8 781 r/min	13 288 r/min	16 197 r/min	17 715 r/min
	105. 24 Hz	146. 35 Hz	221. 46 Hz	269. 96 Hz	295. 25 Hz

Table 9 Undamped critical speeds and mode shapes for midspan part

No.	Bearing stiffness/(N/mm)				
	10^3	2×10^3	5×10^3	8×10^3	10^4
Mode 1	8 976 r/min (149. 59 Hz)	10 197 r/min (169. 96 Hz)	11 168 r/min (186. 13 Hz)	11 446 r/min (190. 76 Hz)	11 542 r/min (192. 37 Hz)
					
Mode 2	20 818 r/min (345. 97 Hz)	27 535 r/min (458. 92 Hz)	36 445 r/min (607. 42 Hz)	40 035 r/min (667. 25 Hz)	41 402 r/min (690. 03 Hz)
					
Mode 3	38 099 r/min (634. 98 Hz)	46 454 r/min (774. 24 Hz)	62 958 r/min (1 049. 29 Hz)	72 959 r/min (1 215. 99 Hz)	77 662 r/min (1 294. 37 Hz)
					

As it could be seen from comparison of the results from Table 8–Table 9 and Table 7 critical speeds for the first ordinal mode of the console part in range of bearing stiffness 10^3 – 2×10^3 N/mm are more close to the first ordinal mode of the full rotor structure with overhang, while critical speeds and mode shapes of the midspan part for the first ordinal mode are more close to ordinal second mode of the full rotor. At the same time in the range of bearing stiffness 8×10^3 – 10^4 N/mm critical speeds of midspan part for the first ordinal mode are closer to the first ordinal mode of the full rotor while critical speeds of the console part are approximately close to the second ordinal mode of the full rotor with overhang. But for the bearing stiffness 5×10^3 N/mm matching is not so clear. Hence it could be said based on comparison of results for separate structures that for the observed rotor model in this paper (Table 7) for the bearing

stiffness lower than 2×10^3 N/mm first ordinal mode would be console mode and second ordinal mode would be first midspan mode due to high motion of the midspan part, at the same time for bearing stiffness higher than 5×10^3 N/mm the order of the mode shapes appearance changes. First midspan mode for the full rotor with overhang becomes first ordinal mode, while console mode becomes second ordinal mode, where midspan part have bending left from previous ordinal mode.

Hidalgo^[3] reveals that console modes or L-modes usually occurs when the difference between the rotor stiffness to mass relation and the overhang stiffness to mass relation is large enough to cause the overhang to act (by itself) as a cantilever beam. Based on the obtained results it could be said that when the overhang part connected with the midspan part and the bearing stiffness is added the mode shape of the

full rotor will correspond to the mode shape of those of its part (console or midspan) whose natural frequency is closer to the current speed of rotor. At the same time with increase of bearing stiffness the natural frequency of the console end increase faster (Table 8) and therefore can quickly become higher than the natural frequency of one of the midspan modes. Hence when considering the full rotor structure the mode order transition can occur.

3.4 Campbell diagram inspection

A very helpful way to understand this phenomenon is to compare the results of Campbell diagram (Fig. 7), where damped critical speeds were calculated for the same rotor with the overhang on the soft and rigid bearings including the mode shapes. As it can be observed the mode shapes are not the same for the mode 1 and mode 2. For the soft bearings mode 1 could be consid-

ered as the console mode due to the high deflections at the overhung end, while at the same time mode 2 is the first midspan mode with the most deflection between the bearings. For the rigid bearings the situation is vice versa, mode shape with the high deflection between the bearings became mode 1 while the console mode travels to the mode 2 but still keeping the bending between the bearings. Calculations have also shown that mode 3 for the soft and rigid bearings was almost the same, with only correction on the motion near the bearings when they are soft, what could be seen from comparison of Table 6 and Fig. 7 results.

4 Influence on rotor balancing

In order to demonstrate the influence of the console mode order change on the rotor when it supposed to be balanced, some calculations were made. The same console rotor was considered to be subjected to initial unbalance which was obtained by summation of distributed unbalances for the first three ordinal modes. To catch the modes transition effect, two cases were modeled. First when the rotor was balanced on the bearings with stiffness 10^3 N/mm suppose for example as at the balancing facility (according to Fig. 3 before the modes transition), and the second case when the already balanced rotor was mounted on more stiff bearings 10^4 N/mm (when the modes transition had already happened). Bearings were isotropic in both cases. Results of numerical simulation for the first case and outcome of balancing procedure are presented in Fig. 8.

From the obtained results it could be seen that distributed unbalance gave rise to three critical speeds, as it was predicted in Table 6. For the front bearing first two critical speeds are more clearly pronounced, while the rear bearing is only subjected to second and third critical speeds. It could be seen that by elimination of the first three modes while balancing procedure simulation the vibration level on the both bearings could be reduced to an acceptable values.

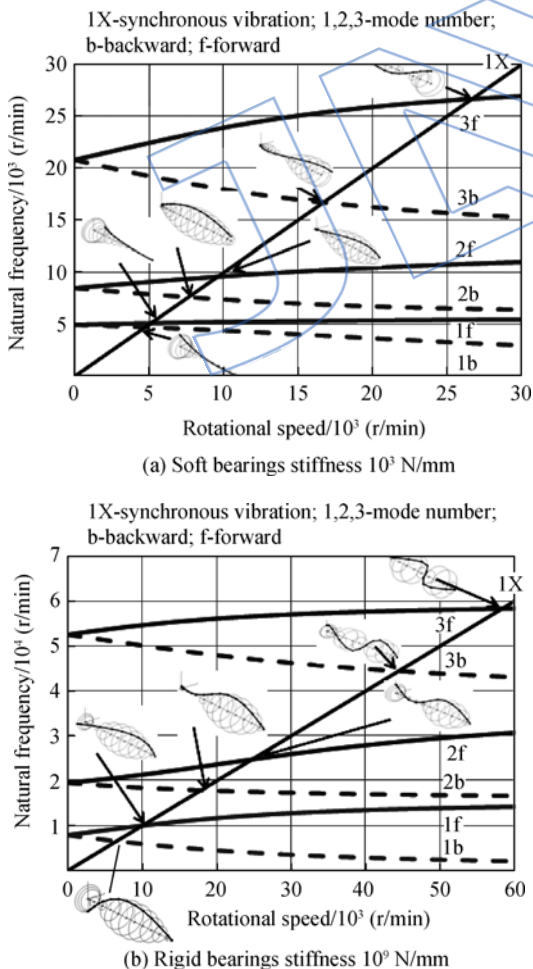


Fig. 7 Campbell diagram

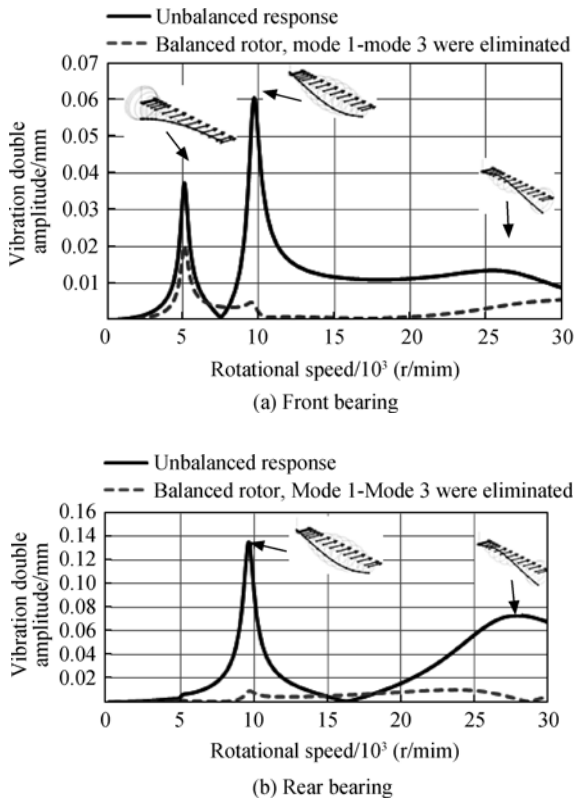


Fig. 8 Results of balancing modeling

At the same manner results of simulation for the second case were presented in Fig. 9. Now the rotor with the same balancing system was mounted on more stiff bearings. It could be seen that although the vibration level for the higher speed modes is even better than before, but for the first critical speed vibration level increased significantly. It happened because the first midspan mode became the first ordinal mode according to the Table 6 results, and the same balancing system which efficiently eliminated console mode when it was first ordinal mode, now only makes it worse. At the same time the third critical speed became higher and beyond the observed speed range.

Examination of the console end vibration (Fig. 10) also showed that vibration level increased significantly when the bearing stiffness was changed. Balancing at the bearings with bearing stiffness 10^3 N/mm decreased vibration level to acceptable value, while further bearing stiffness change brought to significant increase of console end amplitude. Thus obtained results bring to conclusion that the same balancing system

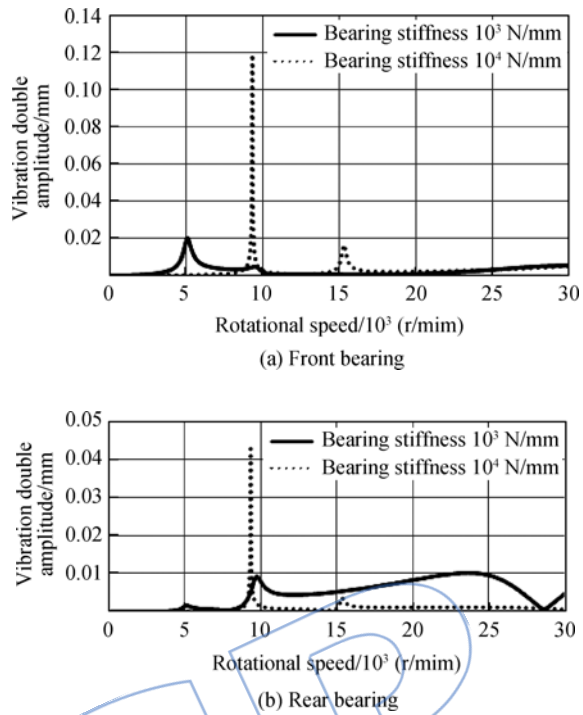


Fig. 9 Results of balanced rotor vibration condition simulation when the bearing stiffness was changed

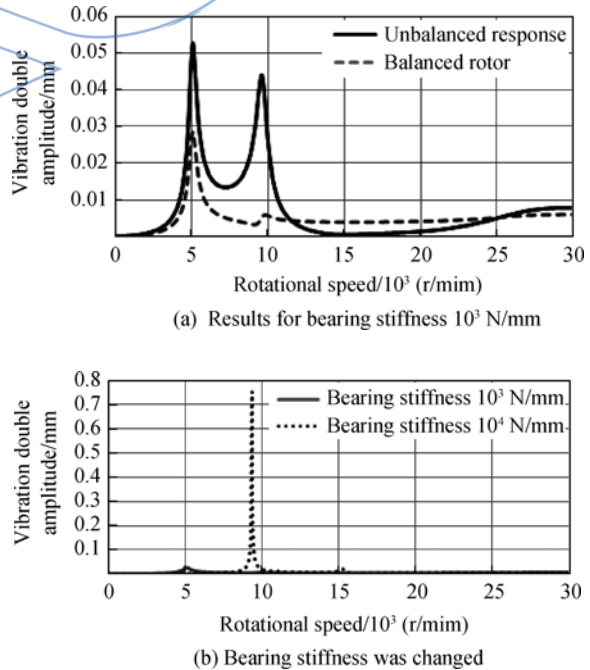


Fig. 10 Vibration response of console end

could not perfectly fit when due to the bearing stiffness vary console modes transition can occur.

To sum up, above described situation of the mode transition or mode order change effect is quite important for implementation of the effec-

tive rotor balancing for the overhang rotors, when the bearing stiffness at the balancing facility is different from the same at the situ or in real machine. What could bring to situation when due to the console mode order change, perfectly balanced at the chamber, in situ would not be so.

One could say that observed situation is quite artificial, and experienced balancing engineer will never let it happen like this. And that is partly true, it was examined mainly to point out what the effect could be. But at the same time another case is possible when the order change could happen for the bearing stiffness equal to the bearing stiffness of the balancing facility or balancing equipment, leading to the event when two different modes are located very close to each other (like in Fig. 3 emphasized by black oval) bringing to difficulties in their recognition and hence further compensation while performing the balancing.

5 Conclusion

Based on the obtained results the following conclusions could be made:

1) The console modes obey the orthogonal principle in the same way as all the other modes and as a consequence could be effectively balanced when the balancing weights are installed considering rotor's bending modes for the corresponding critical speed or near it. It should be pointed out that the order of occurrence for midspan mode shapes for the rotor on two bearings is constant and always executed, hence the mode shapes always follow the classical rule: first midspan mode, second midspan mode, third midspan mode and so on.

2) When the rotor has an overhang the mode transition is possible and could be recognized by presence of the unusual humps on the ordinal mode curves in areas when two modes are close to each other during inspection of the rotor's critical speed map obtained from rotordynamic software. Observation of the critical speed map in this case should be careful since for different bearing stiffness on this map the same or-

dinal modes can have different mode shapes and hence for proper understanding it should be rebuilt taking into account mode shape analysis. Although to receive the exact value of bearing stiffness when the mode order transition happens is complicated due to difficulties in mode shapes recognition, since amplitude of the console end and midspan part could be similar when this stiffness is approached. Nevertheless transition region could be defined and rebuilt critical speed map would be much more informative for engineers while selecting required bearing stiffness, since the behavior of the console mode could be predicted efficiently.

3) Based on the obtained results it can be concluded that when the rotor has an overhang part and midspan part the mode shape of the full rotor is influenced by the mode shapes of its components, like if they are connected in rotor train. Hence the complete rotor will follow the mode shape of those of it part whose natural frequency is closer to the current speed of rotation for the current bearing stiffness.

4) Critical speed analysis together with critical speed map inspection are quite useful before performing balancing procedure of the rotor with overhang especially when the bearing stiffness of the balancing equipment is different from the stiffness at situ.

5) Perfectly balanced rotor could not be so due to modes order transition effect in case when the bearing stiffness is changed. That means that previously installed balancing systems either would not fit to the corresponding mode shape on the critical speeds, or just make the condition of the balancing rotor even worse, what in turn could lead to excessive vibration levels and as a result to damage of the equipment and its parts.

Finally it can be pointed out that modern engineers do not have to always follow the obtained results from the software, but carefully check it based on experience and common sense. Since neglect of rotor's features such as overhangs could bring to problems with their effective balancing and vibration tuning, what in turn

could bring to more dramatic problems such as machine malfunction, failure and increase of costs. Current paper is just a theoretical description of the problem with some simulation examples and more deep work will be performed also in the future based on experimental results confirmation.

References:

- [1] Racic Z, Hidalgo J. Practical balancing of flexible rotors for power generation[C]// Proceedings of ASME, Las Vegas, Nevada, USA: ASME, 2007: 1-10.
- [2] L'vov M M, Gunter E J. Application of rotor dynamic analysis for evaluation of synchronous speed instability of a generator rotor in a high speed balancing facility[C]// Proceedings of ISCORMA-3. Cleveland, OH, USA: [S. l.], 2005: 1-9.
- [3] Hidalgo J I, Dhingra A K. High speed balancing of rotors with overhangs: when is overhang likely to cause problems [J]. Journal of Testing and Evaluation, 2006, 34(3): 1-6.
- [4] Rieger N F. Balancing of rigid and flexible rotors [M]. [s. n.]: The Shock and Vibration Information Center, Stress Technology Inc., 1986.
- [5] Goldin A S. Vibration of rotating machines[M]. Moscow: Mashinostroenie, 2000. (in Russian)
- [6] Muszynska A. Rotordynamics[M]. New York: Taylor & Francis Group, 2005.
- [7] McMillan R B. Rotating machinery: practical solution to unbalance and misalignment [M]. New York: The Fairmont Press Inc., 2004.
- [8] Friswell M I, Penny J E, Lees A W. Dynamics of rotating machines[M]. Cambridge: Cambridge University Press, 2010.
- [9] Uriev E V, Zhukov S V. Investigation on vibration reliability of repair rotors for GTK-25I[J]. Journal of Gas Industry, 2008, 2: 77-82. (in Russian)
- [10] Uriev E V, Shaposhnikov K V. Balancing of the rotors with huge overhangs on the high-speed balancing facilities [J]. Heavy Power Machinery, 2011, 6: 14-21. (in Russian)
- [11] Nelson F D. Rotordynamic without equations[J]. International Journal of COMADEM, 2007, 10(3): 2-10.
- [12] Swanson E, Powell C D, Weissman S. A practical review of rotating machinery critical speeds and modes[J]. Journal of Sound and Vibration, 2005, 5: 10-17.
- [13] Vance J M. Machinery vibration and rotordynamics[M]. Hoboken, New Jersey: John Wiley & Sons Inc., 2010.
- [14] Ehrich F F. Handbook of rotordynamics[M]. New York: McGraw-Hill Inc., 1992.
- [15] Uriev E V. Vibration reliability and turbomachinery diagnostic: Part 1 vibration and balancing[M]. Yekaterinburg: UGTU-UPI, 2005. (in Russian)